Interplay between Magic Number Stabilities and Superfluidity of Small Parahydrogen Clusters

S. A. Khairallah,[1] M. B. Sevryuk,[2] D. M. Ceperley,[3] and J. P. Toennies[4]

[1]*Department of Physics, University of Illinois at Urbana-Champaign, Urbana, Illinois 61801, USA*
[2]*Institute of Energy Problems of Chemical Physics RAS, Moscow 119334, Russia*
[3]*NCSA and Department of Physics, University of Illinois at Urbana-Champaign, Urbana, Illinois 61801, USA*
[4]*Max-Planck-Institut für Dynamik und Selbstorganisation, D-37073 Göttingen, Germany*

(Received 19 December 2006; published 4 May 2007)

The interplay between magic number stabilities and superfluidity of small parahydrogen clusters with sizes $N = 5$ to 40 and temperatures $0.5\ \mathrm{K} \leq T \leq 4.5\ \mathrm{K}$ is explored with classical and quantum path integral Monte Carlo calculations. Clusters with $N < 26$ and $T \leq 1.5$ K have large superfluid fractions even at the stable magic numbers 13, 19, and 23. In larger clusters, superfluidity is quenched especially at the magic numbers 26, 29, 32, and 37 while below 1 K, superfluidity is recovered for the pairs (27, 28), (30, 31), and (35, 36). For all clusters superfluidity is localized at the surface and correlates with long exchange cycles involving loosely bound surface molecules.

DOI: 10.1103/PhysRevLett.98.183401 PACS numbers: 36.40.Mr, 67.90.+z

Hydrogen is the simplest and most ubiquitous of all molecules in the Universe. On the Earth, it plays an important role in many chemical reactions and is presently being developed as an energy transport medium [1]. The $j = 0$ rotational state of the para-H_2 nuclear spin configuration is, like ^{4}He, a spinless boson and below about 6 K has been predicted to be the only naturally occurring superfluid besides the helium isotopes [2]. The observation of superfluidity in the bulk so far has been thwarted by its solidification at 13.96 K. In 1991, Sindzingre *et al.* showed theoretically that small pure clusters with 13 and 18 molecules were superfluid below about 2 K, while larger clusters with 33 molecules had a much smaller superfluid fraction [3]. Later, Grebenev *et al.* observed a superfluid response in small clusters consisting of 15–17 p-H_2 molecules surrounding an oxygen carbonyl sulfide (OCS) chromophore all within a large helium droplet [4]. More recently, magic cluster sizes of pure p-H_2 clusters with $N = 13$, 33, and 55 were observed with Raman spectroscopy in a cryogenic free jet expansion [5]. The earlier calculation of superfluidity in pure H_2 clusters as well as the interpretation of the OCS$(p\text{-}H_2)_n$ experiments have since been confirmed [6,7]. Recently, several groups have reported evidence for magic number stabilities at $N = 13$ [8] and at 23 and 26 with a reduced superfluidity [9].

An intriguing aspect of these studies is the apparent contradiction between the large superfluid fractions and the structured radial distribution functions [10] and the magic number stabilities, which indicate a solidlike rigidity. It is only at high temperatures, when the clusters are molten, that the radial distributions show the same constant interior density and smooth falloff at the surface [3,6] found for superfluid helium clusters which are known to be liquid [11]. This inconsistency has led to the speculation that p-H_2 clusters may be considered as microscopic supersolids [3]. Thus the present study was undertaken to clarify how a cluster which appears to be solid can also be superfluid.

To resolve this apparent incompatibility, both classical and quantum path integral Monte Carlo (PIMC) calculations are reported for all sizes between $N = 5$ and 40 for five temperatures (0.5, 1.0, 1.5, 3.0 K) and the experimentally accessible 4.5 K [12]. The calculations indicate that clusters with $N = 13$, 19, 23, 26, 29, 32, 34, and 37 have highly symmetric structures and show a propensity for stability in agreement with magic number stabilities reported earlier for solid ionized rare gas clusters [13,14]. In the following, these special sizes will be referred to as magic clusters. All the p-H_2 clusters with $N < 26$ have significant superfluid fractions at $T \leq 1.5$ K which are only slightly suppressed in the magic clusters. At magic $N = 26$, superfluidity is greatly quenched and for 29, 32, 34, and 37 reduced even down to $T = 0.5$ K. Clusters with size pairs (24, 25), (27, 28), (30, 31), the singleton 33, as well as (35, 36) show significantly greater superfluid fractions than their more stable magic neighbors. The radial distributions of the superfluid fraction and the distribution of permutation cycle lengths reveal that superfluidity in all the clusters is localized at the surface and for the larger superfluid sizes it correlates with the presence of loosely bound surface molecules. These new results now clarify the apparent contradiction between the structured radial distributions and the large superfluidity found in the previous calculations [3,9].

The calculations were carried out using the PIMC method which is based on the quantum-classical isomorphism where each particle is replaced by a "polymer" made up of M "beads" as explained in detail in Ref. [15]. In the present quantum calculations, a time step of $\tau = 1/80$ was sufficient to obtain converged results within the pair-product approximation. Bose statistics is introduced by cross linking the polymers to form chains of permuting cycles. The classical calculations, which do not account for quantum delocalization, were performed with the semiclassical program of Ref. [16] by making a special choice of certain parameters. Two intermolecular poten-

tials were used: (i) a Lennard-Jones potential with parameters $\sigma = 2.96$ Å and $\epsilon = 34.16$ K and (ii) the more accurate Silvera-Goldman potential. The initial configurations were chosen either from the Cambridge Cluster Database [17] or by carving out a spherical region centered around a molecule in an hcp H_2 crystal. The important effects reported here were independent of the potential and the initial configuration.

Magic classical and quantum clusters were identified by examining the energy differences $\Delta E = E(N, T) - E(N - 1, T)$, where $E(N, T)$ is the total internal energy for a cluster of N molecules at temperature T. The quantity ΔE approaches the chemical potential at $T = 0$; hence, sizes with ΔE values lower than their neighbors are more localized and more tightly bound. Both the classical and the quantum results (presented in Fig. 1) show about the same enhanced relative stabilities at the magic cluster sizes $N = 13$, 19, 23, 26, 29, and 32, indicating that the classical stabilities persist in the quantum clusters. Although 36 and 38 appear to be "magic" in the classical simulation, the expected magic 34 and 37 are found only in the quantum calculations [13,14]. All our quantum calculated magic numbers agree with well-known high symmetry icosahedral-derived structures [13] and have been repeatedly observed in ionized rare gas clusters [13,14]. So far, however, only magic $N = 13$, 33, and 55 have been observed experimentally [5]. Whereas $N = 13$ and 55 correspond to the closing of the first and second icosahedral shells, $N = 33$ is not a magic number among the possible modified icosahedral structures but has a dodecahedral form. Since the experimental resolution [5] was not sufficient to distinguish from the nearby magic 32 and 34, it is possible that the earlier assignment was incorrect—especially if one considers that during cluster growth icosahedral modified structures will be preferred as a result of buildup around the smallest magic $N = 13$ which will be a nucleus for further growth.

The superfluid fraction $\rho_s/\rho_{\text{total}}$ [15] is shown in Fig. 2 as a function of the cluster size and temperature. The nearly 100% fraction in the small clusters decreases sharply above 1.5 K [18]. At each of the magic sizes, $\rho_s/\rho_{\text{total}}$ almost always shows a downward dip reminiscent of those in Fig. 1. These dips are smallest in the small clusters but are more pronounced for $N \geq 26$. Thus, the classical rigidity at the magic sizes suppresses the quantum delocalization needed for superfluidity, an effect which becomes stronger with increasing size. Surprisingly, beyond magic $N = 23$, the superfluid fraction at 1 K jumps back to about unity for the next larger sizes (24, 25). Then beyond magic $N = 26$ a similar rebound occurs for the two lowest temperatures at (27, 28). The minimum at $N = 23$ and two maxima at $N = 25, 27$ were also found in recent calculations by Mezzacapo and Boninsegni [9]. In the present calculations similar maxima are observed at (30, 31) and (35, 36). The singleton $N = 33$ has a very weak rebound and seems to follow the behavior of the neighboring magic sizes as its relatively low binding energy in Fig. 1(b) also suggests. Thus in clusters with solid-like stable structures superfluidity is suppressed, with the largest suppressions found for $N \geq 26$, while at sizes not equal to known magic sizes it is restored. It is interesting that at 1.5 K the interactions are so strong that superfluidity is almost suppressed for clusters $N \geq 26$, yet quantum delocalization in the smaller clusters is still sufficient for their superfluidity.

To understand these unexpected out-of-phase oscillations between magic sizes and superfluid sizes, the three types of radial distributions shown in Fig. 3 were calculated for the magic $N = 26$ cluster and the two adjacent less stable but more superfluid clusters. Figure 3(a) shows the classical distributions at 1.5 K and, as expected, the

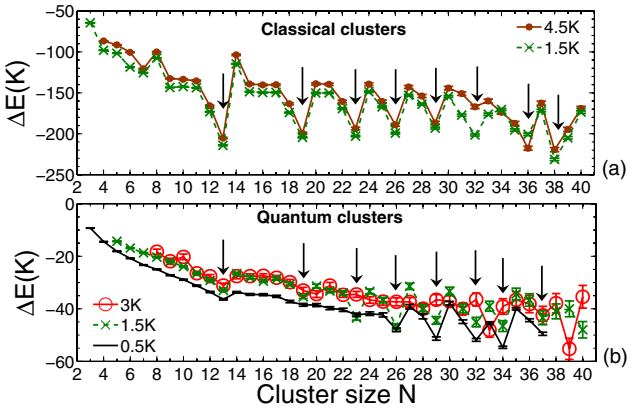

FIG. 1 (color online). Energy differences ΔE as functions of the cluster size calculated classically (a) and with a quantum mechanical PIMC program (b). The sharp minima marked by downward arrows are attributed to especially stable magic icosahedral-derived structures [13,14].

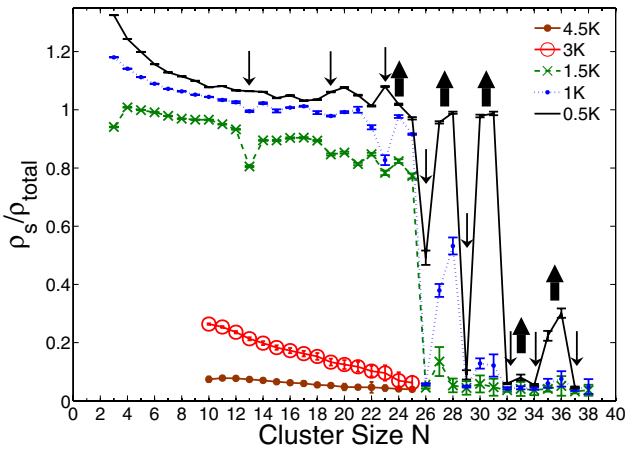

FIG. 2 (color online). The total superfluid density fraction is plotted as a function of the cluster size for five different temperatures. The downward arrows indicate the magic clusters with high symmetry. The upward pointing thick arrows indicate islands of sizes exhibiting enhanced superfluidity. Superfluidity beyond $N = 26$ above 3 K is below 3%.

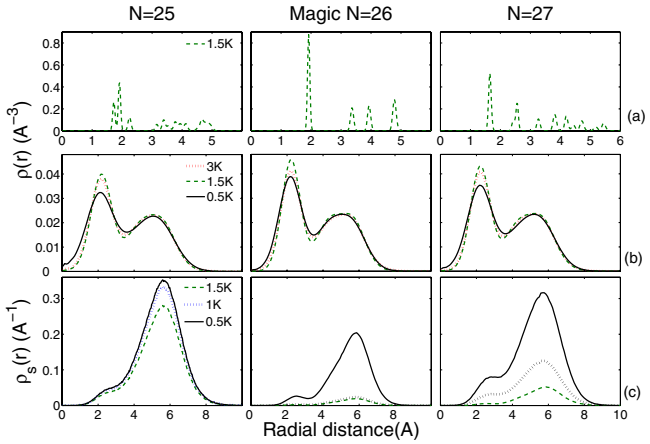

FIG. 3 (color online). Comparison of radial density distributions for the magic cluster $N = 26$ and the neighbors (25, 27) for three characteristic temperatures. The distributions in (a) are classical and those in (b) are from quantum calculations. The radial distributions of the superfluid fraction are plotted in (c). We show only one temperature in (a) since the classical distributions are less sensitive to temperature.

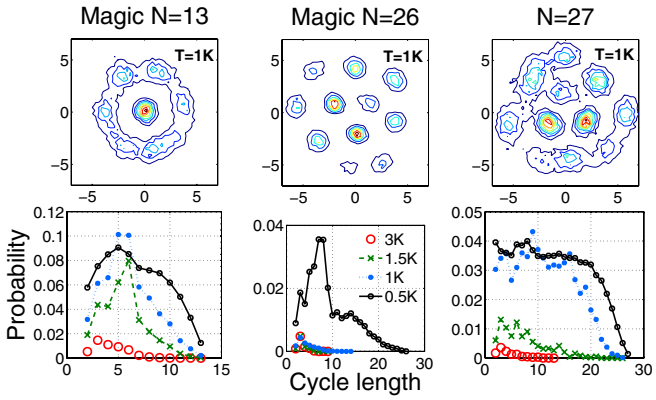

FIG. 4 (color online). Top panels: Density contour plots at $z \approx 0$ plane for magic $N = 13, 26$ and nonmagic $N = 27$. All the lengths are in Å. Bottom panels: The probability distributions for permutations of a given length. The contours for magic $N = 13$ show delocalized molecules at the outer layer that take part in cycles with lengths 5 and 6 which correspond to rings around the central molecule. For magic $N = 26$ at 1 K, all the molecules are highly localized. The surface molecules for $N = 27$ at 1 K are highly delocalized, whereas the core molecules are nearly rigid. This correlates with the long exchange paths around the localized core shown below the contour plot.

molecules for $N = 26$ follow an orderly partitioning into four localized and distinct groups, whereas for $N = 25, 27$ they are randomly distributed. The quantum distributions [Fig. 3(b)] with only two broad peaks show evidence of quantum exchanges between the shells. The magic $N = 26$ cluster has a noticeably larger inner peak compared to its neighbors and also shows a slight dimple in the second outermost peak reminiscent of the classical distribution. The radial dependence $\rho_s(r)$ of the superfluid fraction in Fig. 3(c) is computed by binning the radial location of the beads that are involved in permutation cycles [19]. These distributions exhibit large differences with temperature and with sizes as expected from Fig. 2. Surprisingly, however, the superfluidity is not greatest near the center as found for ^{4}He clusters [11], but is localized at the surface beyond the outer maximum in the radial density distribution. The superfluidity is small in the inner shell especially for magic $N = 26$. We note that the apparent randomness in the classical radial curves [Fig. 3(a)], which is suggestive of less rigid and symmetric structures for the nonmagic $N = 25$ and 27, correlates with the increased superfluid fractions [Figs. 2 and 3(c)].

Additional insight comes from Fig. 4 which provides a cross section view of $N = 13$, 26, and 27 and the probability distributions of the permutation cycles as functions of the permutation length. The contours for $N = 13$ show a considerable delocalization of the outer layer. The $N = 13$ permutation probabilities are dominated by cycles with lengths of 5 and 6 molecules, corresponding to rings around the center, with a relatively high probability of 10% in accordance with the large superfluid fraction (Fig. 2). Even though the central molecule appears to be localized in the contour plot at 0.5 K, it also participates in ring exchanges as indicated by the small $\approx$0.1% probability for cycle exchange lengths of 13. The contour plot for magic $N = 26$ indicates that all its molecules are highly localized and that it is solidlike justifying the greatly suppressed superfluidity (Fig. 2). Contours at different values of z for larger clusters at $T \geq 1.5$ K (not shown) exhibit similar localization. The corresponding permutation probabilities are peaked at very low cycle numbers and are mostly less than 0.05%, which explains their small residual superfluidity in Fig. 2. But as shown by the permutation probabilities, even the magic $N = 26$ melts and becomes superfluid at 0.5 K with a predominance of cycles from 7 to 15. The top panel in Fig. 4 for nonmagic $N = 27$ has a liquid outer layer similar to magic 13 in agreement with Fig. 3(c), but with a smaller peak permutation probability of about 3.5% as expected from its small overall superfluid fraction (Fig. 2). At 0.5 K the permutation probability curve smoothens and extends out to include cycles of 27 molecules suggesting that also the core molecules are participating in the permutations. Thus both the contour plots and probability distributions of the $N = 27$ cluster are consistent with the onset of superfluidity in the surface region.

Recently, Mezzacapo and Boninsegni also observed an enhanced superfluidity for $N = 27$, but their conclusion that "the addition of a molecule to the $N = 26$ has the effect of frustrating the solid order of the inner shell, increasing molecule delocalization and leading to quantum exchanges" [9] is at variance with these new results, which clearly show that superfluidity is at the surface.

The nature of the disorder favoring a large superfluid fraction at the surface emerges from the inherent structure (IS) analysis of Weber and Stillinger [20]: "inherent structures which underlie the liquid state are those stable parti-

cle packings (potential minima) which can be reached by a steepest descent quench on the potential energy hypersurface.'' This quenching procedure eliminates all kinetic effects due to thermal excitations or zero-point motion. In the case of quantum mechanical systems, in the steepest descent minimization, the gradient is to be calculated from the path integral action rather than from the potential. We applied this version of the IS analysis to the p-H_2 clusters in question, with the permutations turned off. The quenched structures are, in general, independent of the temperature [20] and are identical to Wales classical minimum potential energy configurations [17]. This geometric spatial correspondence explains the origin of the persistence of the classical structures in the energy and superfluid densities discussed above.

Among the small cluster sizes, a quenched configuration similar to the Wales body centered icosahedron was quite often found for $N = 13$ indicating that it is particularly stable. Occasionally, quenching would generate variant structures close to the classical ones with some delocalized molecules on the surface suggestive of melting. Clusters differing by one or two molecules from the magic sizes are more often seen to have defective surfaces. Since these clusters differ essentially only in the bonding of the outer molecules, their smaller binding energies (Fig. 2) indicate that these outer molecules are less tightly bound than in the case of the magic clusters. For example, $N = 18$ would statistically appear more often with structures that deviate slightly from the classical clusters, while for magic $N = 19$, almost every IS cluster is the same as the classical cluster. The IS analysis for the other larger superfluid sizes indicates that their surface molecules are also less tightly bound and less ordered.

In summary, our analysis reveals that pure p-H_2 clusters with $N < 26$ at temperatures $T \leq 1.5$ K are liquidlike and have a large superfluid response. It is only somewhat reduced in magic clusters with $N = 13$, 19, and 23, which are classical magic sizes with highly symmetric icosahedral structures. The difference $|\Delta E|$ in internal energies (the energy needed to add one molecule) is less than 38 K for these highly superfluid clusters [Fig. 1(b)]. The larger magic clusters $N = 26$, 29, 32, 34, and 37, in which superfluidity is strongly quenched at $T > 0.5$ K, all have considerably larger internal energy differences of more than $\approx$40 K. Superfluidity is restored in the cluster size pairs (24, 25), (27, 28), (30, 31), the singleton 33, and (35, 36), with smaller $|\Delta E|$ values compared to the magic clusters lying in between. In these superfluid sizes, quantum delocalization of the loosely bound admolecules enables them to explore many different surface structures, thereby favoring large permutation cycles and an increased superfluidity. Our calculations reveal that, with increasing cluster size, the strong many-body intermolecular interactions lead to a rigid solidlike inner core thereby pushing the delocalization-induced superfluidity toward the surface, where it is favored by the reduced coordination and weak inward interaction with the small central core. The overall decay of superfluidity with cluster size and its increased localization on the surface agree with the macroscopic limit of 2D surface superfluidity and zero response in the bulk [21].

We thank Dr. Oleg A. Kornilov and Professor Lev Yu. Rusin for helpful discussions and Professor Victoria Buch for her semiclassical code. This work was supported by NSF (No. DMR-04-04853), NASA (No. NAG-8-1760), and the Deutsche Forschungsgemeinschaft. Computer time was provided by NCSA, the F. Seitz Materials Research Laboratory (U.S. DOE No. DEFG02-91ER45439 and NSF No. DMR-03 25939 ITR) at the University of Illinois, Urbana-Champaign.

[1] http://www.eere.energy.gov/hydrogenandfuelcells/.
[2] V. L. Ginzburg and A. A. Sobyanin, JETP Lett. **15**, 242 (1972).
[3] P. Sindzingre, D. M. Ceperley, and M. L. Klein, Phys. Rev. Lett. **67**, 1871 (1991).
[4] S. Grebenev, B. Sartakov, J. P. Toennies, and A. F. Vilesov, Science **289**, 1532 (2000).
[5] G. Tejeda, J. M. Fernández, S. Montero, D. Blume, and J. P. Toennies, Phys. Rev. Lett. **92**, 223401 (2004).
[6] D. Scharf, G. J. Martyna, and M. L. Klein, Chem. Phys. Lett. **197**, 231 (1992).
[7] Y. Kwon and K. B. Whaley, Phys. Rev. Lett. **89**, 273401 (2002).
[8] S. Baroni and S. Moroni, Chem. Phys. Chem. **6**, 1884 (2005); J. E. Cuervo and P.-N. Roy, J. Chem. Phys. **125**, 124314 (2006); R. Guardiola and J. Navarro, Phys. Rev. A **74**, 025201 (2006).
[9] F. Mezzacapo and M. Boninsegni, Phys. Rev. Lett. **97**, 045301 (2006).
[10] E. Rabani and J. Jortner, J. Phys. Chem. B **110**, 18 893 (2006).
[11] P. Sindzingre, M. L. Klein, and D. M. Ceperley, Phys. Rev. Lett. **63**, 1601 (1989).
[12] E. L. Knuth, F. Schünemann, and J. P. Toennies, J. Chem. Phys. **102**, 6258 (1995).
[13] J. Farges, M. F. De Feraudy, B. Raoult, and G. Torchet, Surf. Sci. **156**, 370 (1985).
[14] W. Miehle, O. Kandler, T. Leisner, and O. Echt, J. Chem. Phys. **91**, 5940 (1989).
[15] D. M. Ceperley, Rev. Mod. Phys. **67**, 279 (1995).
[16] V. Buch, J. Chem. Phys. **100**, 7610 (1994).
[17] http://www-doye.ch.cam.ac.uk/jon/structures/LJ/tables.150.html; D. J. Wales and J. P. K. Doye, J. Phys. Chem. A **101**, 5111 (1997).
[18] Values exceeding 100% in Fig. 2 result from ambiguity in the definition of the moments of inertia in small clusters.
[19] E. W. Draeger and D. M. Ceperley, Phys. Rev. Lett. **90**, 065301 (2003).
[20] T. A. Weber and F. H. Stillinger, J. Chem. Phys. **81**, 5089 (1984).
[21] M. Wagner and D. M. Ceperley, J. Low Temp. Phys. **94**, 161 (1994); **94**, 185 (1994).